

"This is the pre-peer reviewed version of the following article: Valle, J., Burgui, S., Langheinrich, D., Gil, C., Solano, C., Toledo-Arana, A., et al. (2015). Evaluation of Surface Microtopography Engineered by Direct Laser Interference for Bacterial Anti-Biofouling. *Macromolecular Bioscience*, 15(8), 1060–1069., which has been published in final form at <http://doi.org/10.1002/mabi.201500107>. This article may be used for non-commercial purposes in accordance with [Wiley Terms and Conditions for Self-Archiving](#)."

1 Evaluation of Surface Microtopography Engineered by 2 Direct Laser Interference for Bacterial Anti-Biofouling

3 Jaione Valle^{1*}, Saioa Burgui¹, Denise Langheinrich^{2,3}, Carmen Gil¹, Cristina Solano¹, Alejandro
4 Toledo-Arana¹, Ralf Helbig⁴, Andrés Lasagni^{2,3}, Iñigo Lasa^{1*}

5
6
7
8
9
10
11
12 ¹Laboratory of Microbial Biofilms. Instituto de Agrobiotecnología, INAMAT. Universidad
13 Pública de Navarra-CSIC-Gobierno de Navarra. Campus de Arrosadía. Pamplona, Spain.

14
15 ²Fraunhofer Institute for Material and Beam Technology (IWS) Dresden, Winterbergstraße 28,
16 01277 Dresden, Germany.

17
18
19 ³Institute for Manufacturing Technology, TU Dresden, George-Bähr-Straße 3c, 01069 Dresden.

20
21 ⁴Leibniz Institute of Polymer Research (IPF) Dresden, Hohe Straße 6, 01069 Dresden.

22
23
24
25
26
27
28
29
30
31
32
33
34
35
36
37
38
39
40
41
42
43
44
45
46
47
48
49
50
51
52
53
54
55
56
57
58
59
60
61
62
63
64
65

18 * Corresponding author. Jaione Valle and Iñigo Lasa.

19 Laboratory of Microbial Biofilms. Instituto de Agrobiotecnología, UPNA-CSIC. Campus de
20 Arrosadía s/n. Universidad Pública de Navarra-31006. Pamplona. Spain

21 Email: jaione.valle@unavarra.es, ilasa@unavarra.es

23 **Abstract**

1 24 Biofilm formation by bacterial pathogens on the surface of medical and industrial settings is a
2
3 25 serious health problem. Modification of the biomaterial surface topography is a promising
4
5 26 strategy to prevent bacterial attachment and biofilm development. However, fabrication of
6
7 27 functional biomaterials at large scale with periodic network-topology is still problematic. In this
8
9 28 study, we use direct laser interference (DLIP), an easily scalable process, to modify polystyrene
10
11 29 surface (PS) topography at sub-micrometer scale. The resulting structure surfaces were
12
13 30 interrogated for their capacity to prevent adhesion and biofilm formation of the major human
14
15 31 pathogen *Staphylococcus aureus*. The results revealed that three-dimensional micrometer
16
17 32 periodic structures on PS have a profound impact on bacterial adhesion capacity. Thus, line-
18
19 33 and pillar-like topographical patterns enhanced *S. aureus* adhesion, whereas complex lamella
20
21 34 microtopography reduced *S. aureus* adhesion both in static and continuous flow culture
22
23 35 conditions. Interestingly, lamella-like textured surfaces retained the capacity to inhibit *S. aureus*
24
25 36 adhesion both when the surface is coated with human serum proteins *in vitro* and when the
26
27 37 material is implanted subcutaneously in a foreign-body associated infection model. Our results
28
29 38 establish that the DLIP technology can be used to functionalize polymeric surfaces for the
30
31 39 inhibition of bacterial adhesion to surfaces.
32
33
34
35
36
37
38
39
40
41
42
43
44
45
46
47
48
49
50
51
52
53
54
55
56
57
58
59
60
61
62
63
64
65

43 1. Introduction

1 44 One of the major challenges of materials engineering discipline is to generate surfaces
2
3
4 45 preventing bacterial adhesion by repelling bacterial cells from attaching (antibiofouling) or
5
6 46 alternatively, inactivate the bacteria in contact with the surface (bactericidal surfaces) ^[1].

7
8 47 Colonization of the surface with bacteria has in most cases an adverse effect on the
9
10
11 48 functionality of the interface, such as clogging of industrial pipes and tubing, decreased
12
13 49 performance of shipping vessels, contamination of food manufacturing surfaces and medical
14
15 50 implants. The strategies to prevent and combat bacterial adhesion and proliferation to abiotic
16
17
18 51 surfaces include chemical modifications with antibacterial agents (antibiotics, antimicrobial
19
20
21 52 peptides, alkyl chains, metals, detergents) and physical modification of the surface topography
22
23 53 ^[2,3]. Because chemical modifications very often lead to toxicity due to the release of the
24
25
26 54 chemical compounds and rapid selection of resistant bacteria, the role of surface topography in
27
28 55 creating surfaces with antibiofouling properties is receiving greater consideration ^[4,5]. The idea
29
30
31 56 is to produce three-dimensional (3D) topographical patterns on the surface that result in reduced
32
33 57 contact area so that bacteria are forced to span the distance between structures to generate
34
35 58 productive interactions. Obviously, modification of the surface topography can be combined
36
37
38 59 with chemical coating of the surface with antibacterial agents.

39
40 60 Initial approaches to explore the effect of surface topography on bacterial adhesion were carried
41
42
43 61 out by mechanical roughening and polishing techniques, generating random texturized
44
45 62 roughness surfaces that modulate bacterial adhesion ^[6-11]. More recently, micropatterning
46
47
48 63 techniques such as optical lithography, microcontact printing, electron or ion beam lithography
49
50 64 that allow the fabrication of periodic microstructures with well-defined and reproducible
51
52 65 dimensions and shapes, have been used ^[12,16]. However, these techniques require multiple steps
53
54
55 66 and long processing times to produce surface geometries, especially if large areas have to be
56
57
58 67 processed. As a complementary alternative to these methods, the Direct Laser Interference
59
60 68 Patterning (DLIP) technology provides a new strategy to generate periodic micro- and

69 nanotopographies on different polymeric and other substrates. This method enables the large-
70 scale fabrication of complex structures by systematically varying the dimensions of the gratings
71 superimposed upon each other. Another significant advantage of DLIP compared with other
72 surface patterning methods is that fairly large areas can be processed within a short period of
73 time (up to several cm^2/s) using single or multiple laser pulses ^[17].

74 Biofilms represent the normal form of bacterial life in natural environments. In biofilms,
75 bacteria grow attached to the inert surface or living tissue and embedded in an extracellular
76 matrix that protects bacteria from environmental stresses, predators, antimicrobials or the
77 immune system ^[18]. Biofilm formation starts with irreversible attachment of planktonic bacteria
78 to the surface, a process that is mediated by physical forces or specific interactions. Then,
79 sessile bacteria divide and secrete an extracellular matrix that anchors bacteria firmly to the
80 substrate and among them. Finally, single bacteria or cell clusters can actively disintegrate from
81 the biofilm or passively be shed through mechanical disruption ^[19-21]. *Staphylococcus aureus*,
82 together with *Staphylococcus epidermidis*, are the most significant gram positive bacterial
83 pathogens that can form biofilms on medical devices such as catheters, valves, prostheses and
84 port-A-caths ^[20,22]. *S. aureus* from skin and mucous membranes from healthy humans can
85 adhere to the surface via nonspecific interactions based on the physicochemical properties of
86 the cell enveloped or through specific binding between compounds of the cell envelop and
87 proteins of the host serum coating the surface of the implanted material. Living inside the
88 biofilm increases bacterial resistance to the action of the immune system and antimicrobials. As
89 a consequence, staphylococcal biofilm associated infections are difficult to eradicate and in
90 most cases the contaminated implants need to be removed to cure the infection.

91 In this study, polystyrene polymer surfaces were patterned with periodical line- (1D), pillar-like
92 (2.5D) and a complex combination of lamella- and line-like pattern (3D) by applying the Direct
93 Laser Interference Patterning (DLIP) technique. After patterning, those samples together with
94 non-patterned substrates of the same materials were used for *Staphylococcus aureus* bacterial

95 adhesion tests *in-vitro* under static and continuous flow conditions as well as in an *in-vivo*
1 96 infection model. The results revealed that line- and pillar-like patterns promote *S. aureus*
2
3 97 adhesion whereas lamella-like patterns reduce bacterial adhesion in steady state and continuous
4
5 98 flow conditions. *In-vivo* testing of lamella-patterned polymers demonstrated the potential of this
6
7
8 99 microtopography to reduce staphylococcal biofilm on implanted materials.
9

10
11 100

14 101 **2. Materials and methods**

16 102 *2.1 Patterning of polymeric materials*

18 103 We used commercially available polymeric materials purchased from Goodfellow GmbH (Bad
19
20 104 Nauheim, Germany). Two different polystyrene (PS) substrates with a thickness of 125 μm
21
22 105 (biaxial orientated) and 1.2 mm were used. The samples were patterned using a high-power
23
24
25 106 pulsed, frequency quadrupled Nd:YAG laser (Quanta Ray, Spectra Physics) emitting a beam
26
27 107 with a wavelength of $\lambda = 266$ nm. The samples were irradiated with 10 ns pulses at a frequency
28
29 108 of 10 Hz. For obtaining 1D line-like structures the two beam experimental set-up was used
30
31 109 which is described elsewhere ^[23]. The spatial period Λ was varied from 1 to 5 μm by keeping a
32
33 110 constant wavelength of $\lambda = 266$ nm and varying the incident angle 2α between the two laser
34
35
36 111 beams following:

$$41 \quad \Lambda = \frac{\lambda}{2 \sin \alpha}$$

44 112 For obtaining a 2D structure (e.g. pillars), the samples were rotated by an angle of 90° between
45
46 113 two subsequent laser shots. All experiments were performed at ambient conditions of pressure
47
48
49 114 and temperature.
50

53 115 *2.2 Bacterial strains and animals manipulation*

55 116 *S. aureus* 15981 was isolated at the Microbiology Department of the Clínica Universidad de
56
57 117 Navarra (Pamplona, Spain) ^[24]. Staphylococci were cultured on tryptic soy agar (TSA) or broth
58
59 118 (TSB) at 37 °C supplemented with glucose (0.25 %) or with human serum (10 %) when
60
61
62
63
64
65

119 indicated. All animal studies were reviewed and approved by the Comité de Ética,
120 Experimentación Animal y Bioseguridad, of the Universidad Pública de Navarra (approved
121 protocol PI-019/12). The work was carried out at the Instituto de Agrobiotecnología under the
122 principles and guidelines described in European Directive 86/609/EEC for the protection of
123 animals used for experimental purposes.

124 *2.3 Bacterial attachment and biofilm formation*

125 For the analysis of *S. aureus* adhesion under static conditions, an overnight culture of *S. aureus*
126 was diluted with a ratio of 1:100. Two ml of the diluted cultured were added to 6-well
127 microtiter plate. Substrates of 2 x 2 cm² from all patterned and non-patterned (reference)
128 polymer surfaces were put in each well and plates, which were incubated for 2 hours at 37 °C
129 with shaking. After incubation, the substrates with the attached bacteria were removed from the
130 microtiter plate culture with tweezers, gently rinsed three times with sterile PBS non-adherent
131 bacteria.

132 The biofilm formation under continuous flow conditions, tested on polystyrene surfaces, was
133 performed using 60-ml microfermenters (Pasteur Institute, Laboratory of Fermentation) with a
134 continuous 40 ml h⁻¹ flow of medium and constant aeration with sterile compressed air
135 (0.3 bar)^[25]. Polystyrene wafers (1 x 1 cm²) of the patterned surfaces as well as non-patterned
136 surfaces as reference were fixed on glass slides, which were then submerged in the
137 microfermentor. Approximately 10⁸ bacteria from an overnight culture of *S. aureus* 15981 were
138 used to inoculate the microfermenters and were then kept at 37 °C for 6 h.

139 For both analyses, after incubation the substrates with the attached bacteria were removed from
140 the microtiter plate and microfermentor, respectively, gently rinsed three times with sterile PBS
141 and then placed in 1 ml of PBS and vigorously vortexed. Subsequently, the samples were
142 serially diluted and plated onto TSA plates for enumeration of viable staphylococci (colony
143 forming units, CFU) and biofilm morphology analysis. The relative adhesion was calculated as
144 bacterial counts CFU on patterned surfaces / CFU on non-patterned surfaces.

145 2.4 Visualization and topographical characterization

146 A scanning electron microscope (Philips XL30 ESEM-SEG) with an operating voltage of 5 kV
147 was used for visualizing the surface of the patterned sample as well as the attached bacteria. A
148 thin gold coating of several nm was sputtered on the non-conductive samples to avoid charge
149 processes. The topographical analysis (structure quality and depth) was conducted with a
150 confocal microscope (Leica DCM 3D) using a 150x objective with a lateral and z-resolution of
151 150 nm and 4 nm, respectively. For the epifluorescence analysis polystyrene wafers were
152 incubated with *S. aureus* 15981 expressing the green fluorescence protein GFP for 4 h under
153 static conditions. A wide-field fluorescence microscopy was used for imaging of the cells
154 attached to the PS surfaces. Each surface was visualized using a 100x oil immersion lens and 10
155 fields of view were randomly chosen for statistical analysis.

156 2.5 In-vivo model of polymeric-associated biofilm infection.

157 For the *in-vivo* model, patterned and non-patterned substrates with a size of 0.5 x 0.5 cm² were
158 used. Two different analyses were performed: bacterial contamination on the PS substrates (i)
159 prior and (ii) post implantation. For the prior-implantation tests, the substrates were incubated
160 with 0.5 ml of 1:100 overnight dilution of *S. aureus* 15981 culture for 1 hour at 37 °C with
161 shaking. The *in-vivo* tests with post-implantation contamination were performed with sterile PS
162 substrates. For both analyses, CD1 mice were anesthetized by intraperitoneal injection of a
163 ketamine/xylazine mixture. After abdominal epilation and antisepsis of the operative field, the
164 animals were operated. An incision of 1.5 cm in the skin was performed with displacement of
165 the subcutaneous space and opening of the peritoneal cavity. Then, contaminated and non-
166 contaminated respectively polymeric surfaces were fixed at the abdominal wall. The peritoneal
167 cavity was closed by suture with 6/0 Monosyn[®]. The animals were put in a warm environment
168 and when awake back in their cages. Within the post-implantation tests, a bacterial suspension
169 containing 10⁸ bacteria of *S. aureus* 15981 was injected two days after surgery intraperitoneally
170 at the site of the polymer implantation. After 5 days, all animals were sacrificed and the

171 polymeric substrates were extracted and placed in 1 ml of PBS and vigorously vortexed. The
172 samples were serially diluted and plated onto TSA plates for enumeration of viable
173 staphylococci. The relative adhesion was calculated as bacterial counts CFU on patterned
174 surfaces / CFU on non-patterned surfaces.

175 *2.6. Statistical analysis*

176 Statistical analysis was performed by one-way analysis of variance combined with the
177 Bonferroni multiple post-hoc test or by the Mann-Whitney test, with $P \leq 0.05$ considered
178 significant (GraphPad InStat, version 5).

179 **3. Results**

180 *3.1. Design of patterned surfaces by DLIP*

181 To analyze whether microstructures generated with Direct Laser Interference Patterning (DLIP)
182 technique on the surface of polystyrene (PS) polymers can modify bacterial adhesion capacity,
183 we generated surfaces with different microtopography geometries. We used spatial grating
184 periods (Λ) varying from 1 and 5 μm and a laser fluence that was adapted to obtain the optimal
185 structure quality (e.g. avoiding collapse of the fabricated array) depending on the spatial period
186 (Table 1). PS wafers with 1.2 mm thicknesses were patterned with periodic line (LN) and pillar
187 (PL) foils with maximal achievable structure depths of $d_{\text{struc}} = 1.63 \pm 0.09 \mu\text{m}$ and
188 $d_{\text{struc}} = 1.85 \pm 0.1 \mu\text{m}$ respectively (Figure 1A). Scanning electron microscopy analysis of PS
189 surfaces patterning with LN and PL revealed a well-defined, reproducible and homogeneous
190 pattern of lines and pillars with precise edges (Figure 1A and B). A similar laser treatment on
191 thin PS films (125 μm thickness) creates a combination of a lamella microtopography (LA)
192 with a 2.0 μm spatial period ($d_{\text{struc}} = 0.47 \pm 0.02 \mu\text{m}$) and a line-like structure with periodicities
193 of 6 or 8 μm ($d_{\text{struc}} = 4.33 \pm 0.06 \mu\text{m}$) (Figure 1A and B). The lamella microtopography results
194 from partially collapsing line-like features due to the lower mechanical stability of the thin PS
195 film compared to the thicker one. The results indicate that DLIP can be used to fabricate 1D to
196 3D micropatterns on PS polymers.

197 *3.2 Quantitative analysis of S. aureus adhesion to the patterned surfaces.*

198 The clinical strain *S. aureus* 15981 was selected to evaluate the impact of surface
199 microtopography on *S. aureus* adhesion capacity. *S. aureus* 15981 produces high levels of β 1-6
200 linked poly-N-acetylglucosamine (PIA/PNAG) and it is accepted as a prototype strain of
201 exopolysaccharide-dependent biofilm formation [24]. Polystyrene wafers with patterned and
202 non-patterned surfaces were incubated with bacteria in TSB-gluc media. After 2 hours, the
203 number of bacteria attached to the surface was determined by serial dilution and plating. The
204 results revealed that line- and pillar-like microtopographical patterns enhanced *S. aureus*
205 adhesion to PS polymeric materials (Figure 2A and B). In particular, a spatial period of 1 μ m
206 induced higher bacterial attachment ($P < 0.05$) than periods of 5 μ m. In contrast, the lamella-like
207 topography on the thin PS substrates (LA) caused a significant reduction on the adhesion of *S.*
208 *aureus* compared to non-patterned PS surfaces (CT) (Figure 2C). These results revealed that
209 microtopographical patterns on PS have a profound impact on *S. aureus* adhesion.

211 *3.3 Qualitative evaluation of bacterial attachment on PS polymers*

212 Because enumeration of bacteria cannot distinguish between monolayers, where most of the
213 bacteria are in contact with the surface, or scattered aggregates, where only few bacteria are in
214 contact with the surface, we used epifluorescence microscopy and scanning electron
215 microscopy to evaluate the adhesion behavior. As it is shown in Figure 3A, large aggregates of
216 bacteria attached to PL and LN surfaces were visualized by immunofluorescence. Bacterial
217 aggregates adhered not only to the top of the structure but also inside the features. These
218 attachment patterns suggest that bacteria respond to the surface topography by maximizing the
219 contact area with the surface. In contrast, few bacteria randomly oriented along the surface were
220 attached on LA patterned surface. Strikingly, single or small aggregates of bacteria were
221 attached to the non-modified PS surface (CT) (Figure 3A).

222 This behavior was confirmed by SEM analysis. The micrographs of patterned surfaces
223 incubated with *S. aureus* revealed large bacterial aggregates on PL polystyrene surfaces, while
224 only individual bacteria or small bacteria clusters/aggregates scattered on the surface of both
225 the LA and the non-treated materials were observed, respectively (Figure 3B).

226 3.4 Bacterial attachment to patterned surfaces under flow-continuous conditions

227 *S. aureus* attachment to patterned polystyrene surfaces was assessed under continuous flow
228 conditions using microfermenters^[25]. The flow rate of fresh medium (40 ml h⁻¹) imposed in the
229 process was high enough to avoid any significant planktonic growth (Figure 4A). Polystyrene
230 substrates of 1 x 1 cm² of PL, LA and non-patterned surfaces were fixed on the glass slides
231 present inside the microfermenter (Figure 4B). *S. aureus* 15981 strain was inoculated in the
232 microfermenters and incubated for 6 hours. In agreement with the results obtained under static
233 conditions, LA-patterned substrates significantly reduced the adhesion of *S. aureus* compared to
234 the non-patterned surfaces (P<0.01) (Figure 4C). Furthermore, PL microtopography increased
235 the adhesion of *S. aureus* to patterned surfaces (Figure 4C).

236 Once a surface is implanted in a living body and comes into contact with biological fluids, such
237 as blood or serum, the proteins present in the media immediately coat the medical device.
238 Numerous studies indicated that coating of the medical devices with host factors facilitate *S.*
239 *aureus* attachment and biofilm formation^[1,26]. To address whether coating of the
240 micropatterned surface with plasma proteins has an impact on the capacity of *S. aureus* to
241 attach irreversibly to the surface, we measured the adhesion capacity of bacteria to LA
242 substrates preincubated with human serum under flow conditions. For that, LA polystyrene
243 surfaces preincubated with media supplemented with human serum (10 %) for 1 h inside the
244 microfermenter, were inoculated and incubated for 6 h with bacteria. Enumeration of the
245 bacteria attached to the LA surface revealed a small but significant decrease compared to the
246 bacteria attach to the non-patterned surface (Figure 4D). These results indicated that lamella

247 microtopography can efficiently reduce *S. aureus* adhesion under flow continuous conditions
248 even in the presence of serum proteins.

249 3.5 *In-vivo* biofilm formation model on PS surfaces

250 Although *in-vitro* assays have proven effective at identifying mechanisms involved in bacterial
251 attachment and biofilm accumulation, it is important to validate the significance of these assays
252 *in-vivo*. Thus, we tested the efficacy of LA microtopography to reduce *S. aureus* attachment
253 and biofilm development using a biofilm infection model in two alternative scenarios. First, LA
254 and control surfaces pre-coated with 10^4 CFU of *S. aureus* 15981 were implanted in the
255 intraperitoneal cavity of mice (Figure 5A). After five days, animals were sacrificed, to
256 aseptically removed the polystyrene wafers and evaluate the bacterial load (Figure 5B). We
257 found that LA surfaces showed a lower degree of colonization than the non-patterned surface
258 ($P<0.05$) (Figure 5C).

259 Second, sterile LA and non-patterned PS surfaces were implanted into the mice and two days
260 after surgery, contaminated with 10^4 CFU of *S. aureus* 15981. Enumeration of *S. aureus* cells
261 attached to the PS wafers 5 days after infection showed that LA surfaces displayed a
262 significantly lower colonization compared to non-patterned surfaces ($P<0.01$) (Figure 5C).
263 Thus, PS-LA wafers displayed a lower level of colonization than non-patterned PS surfaces *in-*
264 *vivo*.

266 4. Discussion

267 Bacterial-surface interactions are governed by multiple factors including surface topography as
268 one of the most important. Three parameters of surface roughness, which have been regularly
269 evaluated for the impact on bacterial adhesion, are the spacing of the trenches, the pattern
270 regularity and the feature shape. Since most of the bacterial cells are in the micrometer size
271 range and their surface appendages are in the nanometer size range, changes of the space at the
272 range of nanometer to micrometer size may disturb bacterial attachment by promoting or

273 reducing cell adhesion. Initial investigations reported that surface features in the range of
274 bacterium size allowed for maximization of the bacteria–surface contact area, hence increasing
275 cell attachment ^[2,3,7,27], whereas surface with topographic features smaller than the diameter of
276 bacterial cells display a small accessible surface area ^[4,5,28]. In this case, bacterial extracellular
277 appendages such as flagella, pili and fimbriae would be responsible for bacterial adhesion as
278 they can interact with nanoscale features ^[6-11,29,30]. With respect to the pattern uniformity,
279 several studies showed that bacteria prefer to align and grow on uniform patterns compared to
280 irregularly distributed or non-patterned surfaces ^[12-16,31-35]. Finally, feature shape could also
281 impact on the bacterial attachment. For instance, surfaces with protruding square features repels
282 bacterial adhesion to the top of the squares independently of the dimensions of the valleys ^[17,36].
283 In addition, surfaces equipped with arrays of hexagonal features significantly reduced *E. coli*
284 initial attachment at short exposure times, whereas this behavior reverses to increase adhesion
285 at longer exposures probably because surface appendages enables bacteria to overcome
286 unfavorable surface topographies ^[18,30]. Other studies used microtopographies inspired in
287 natural surfaces with antibacterial properties (plant leaves, animal skin and insect wings) to
288 reproduce their behavior ^[1,19-21]. An example of a natural inspired antibacterial surface was
289 based on shark skin. This topography was not efficient to inhibit bacterial attachment in the size
290 range of 1–2 μm but it was effective at physically disrupting further colonization and
291 subsequent biofilm development ^[20,22,37]. In conclusion, despite of the considerable amount of
292 information generated over the years, bacterial adhesion in response to surface
293 microtopography is still largely empirical since every surface topography present unique
294 challenges.

295 The results obtained in this study demonstrated that pillar (PL) and line (LN) microtopographic
296 features in the range between 1 to 5 micrometers increased bacterial adhesion to PS surface
297 comparing with non-patterned ones. Furthermore, feature with spatial period of 1 μm , which is
298 close to the diameter of *S. aureus* cells (0.6 – 1 μm), considerably induced a higher bacterial

299 attachment to PS (Figure 2) but also to polyimide (PI) and poly(ethylene terephthalate) (PET)
300 polymers (supplementary Figure 1). In contrast, a complex lamella microtopography (LA)
301 strongly inhibited bacterial adhesion. This topography combines line-like patterns of 2.5 μm
302 feature width and periodicities of 6 or 8 μm with lamella-like patterns of approximately 1.0 μm
303 feature width and periodicities of 2 μm . The molecular reason why lamella microtextured
304 reduced the capacity of *S. aureus* to establish productive contacts with the surface, both under
305 static and flow conditions, remains unknown.

306 The methods used to produce repetitive surface topographies such as optical lithography,
307 electron or ion beam lithography and laser writing, normally require multiple steps and long
308 processing times to fabricate the final micro- and submicrometer surface ordered. DLIP has
309 been previously used to fabricate periodic structures with micrometer and submicrometer
310 patterned topography on large-area of different polymers, metals, ceramics and coatings ^[23,38].
311 In this study, we selected PS because this is one of the most popular biomaterial used for a wide
312 range of medical applications, including diagnostic instruments, medical devices, implants,
313 disposable laboratory ware and tissue culture components ^[24,39]. Treatment of PS with the UV-
314 laser caused photo-thermal based ablation ^[25,40]. As a consequence, a zone of molten or soften
315 material (in addition to volatile products) is produced at the positions of the intensity maxima.
316 Due to the high pressure of the volatile material, the soften material is pulled out toward the
317 positions of intensity minima where it re-solidifies. This leads to a more round shaped structure
318 morphology. Besides, depending on the thickness of PS material, two different topographies
319 were observed during the two-step irradiation process. The characteristic PL geometry observed
320 for the thick PS material results from the local ablation process at the interference maxima
321 positions. In the first irradiation step, the LN geometry is obtained which later evolves into the
322 PL pattern after rotation of the sample (90°) and subsequent irradiation step. In contrast, a
323 similar treatment on the thin PS material results in a more complex topography. In this case, the
324 first irradiation process generates the characteristic 2.0 μm geometry whereas the second

325 irradiation process causes a partial collapsing of the line and creates the 6-8 μm perpendicular
1 326 lamella features. So far, the LA-microtopography has only been obtained in PS polymers,
2
3 327 though efforts are being made in order to obtain the same topographic pattern on PI and PET
4
5 328 polymers.
6
7 329 Multiple studies have examined the effect of surface topography on bacterial adhesion under
8
9 330 static conditions. On the contrary, few works have explored the effect of fluid flow on bacterial
10
11 331 attachment on engineered surfaces ^[14,24,28]. We have used continuous flow culture bioreactors
12
13 332 with a 40 ml h⁻¹ flow rate to evaluate the effect of LA-like topography on bacterial adhesion.
14
15 333 The results showed that this topography reduced *S. aureus* adhesion under shear stress
16
17 334 conditions significantly more effectively than in steady state conditions, suggesting that the
18
19 335 flow of fluid over the surface removes more easily bacteria from the lamella-texturized surface
20
21 336 ^[25,28]. Additional studies will be required to investigate lamella-like topography performance
22
23 337 under flow conditions.
24
25 338 Once a biomaterial is implanted in a living body, coating by blood or other human fluids may
26
27 339 alter the susceptibility of the material to inhibit bacterial adhesion and biofilm formation.
28
29 340 Interestingly, lamella-like topography is still able to reduce *S. aureus* adhesion to PS surfaces in
30
31 341 the presence of human serum, though the reduction was less pronounced. In agreement,
32
33 342 experiments with animal models showed that polystyrene surfaces with lamella
34
35 343 microtopography reduced *S. aureus* colonization and biofilm formation on PS surfaces after 5
36
37 344 days independently of whether the infection has occurred during the surgical procedure or post-
38
39 345 implantation. These results indicated that surface microtopography showed encouraging
40
41 346 efficacy to reduce *S. aureus* attachment and biofilm development *in vivo*.
42
43 347 In summary, these results illustrate that the flexible DLIP technology can be used to develop
44
45 348 engineered microtopographies on polystyrene to reduce adhesion and biofilm formation of *S.*
46
47 349 *aureus*. Polystyrene surfaces composed of lamella-like texture might provide a promising
48
49 350 strategy to reduce *S. aureus* adhesion to biomedical surfaces.
50
51
52
53
54
55
56
57
58
59
60
61
62
63
64
65

351 **5. Conclusions**

1 352 In this paper we illustrate that the flexible DLIP technology can be used to develop engineered
2
3 353 microtopographies on polystyrene polymers. The resulting microtopographies have a profound
4
5 354 impact on *S. aureus* adhesion capacity indicating that surface topography represents a
6
7
8 355 promising strategy to reduce *S. aureus* attachment and biofilm development on the surface of
9
10 356 indwelling medical devices.

11
12
13 357 However, because our knowledge about the influence of surface microtopography on bacterial
14
15 358 adhesion is still largely empirical, it is necessary to experimentally test every pattern to
16
17
18 359 determine its behavior under both *in vitro* and *in vivo* conditions. In our study, regular line and
19
20 360 pillar-like patterns enhance *S. aureus* adhesion whereas a irregular lamella microtopography
21
22 361 reduces adhesion both in static and continuous flow culture conditions. Moreover, lamella-like
23
24
25 362 textured surfaces inhibit *S. aureus* adhesion in the presence of human serum proteins and when
26
27 363 the material is implanted subcutaneously in a foreign-body associated infection model. Ongoing
28
29 364 research is necessary to demonstrate that lamella microtopography on the surface of other
30
31 365 polymers, such as polyimide and poly(ethylene terephthalate), also inhibits *S. aureus* adhesion.
32
33
34

35 366
36
37
38
39
40
41
42
43
44
45
46
47
48
49
50
51
52
53
54
55
56
57
58
59
60
61
62
63
64
65

367 **Acknowledgements**

1 368 J. Valle was supported by Spanish Ministry of Science and Innovation “Ramón y Cajal”
2
3 369 contract. This research was supported by grants AGL2011-23954 and BIO2011-30503-C02-02
4
5 370 from the Spanish Ministry of Economy and Competitiveness and IIQ14066.RI1 from Innovation
6
7
8 371 Department of the Government of Navarra. A. Lasagni, D. Langhenrich and R. Helbig thank
9
10 372 the Deutsche Forschungsgemeinschaft (DFG) for the financial support of the project
11
12 373 “Mechanically stable anti-adhesive polymer surfaces” (LA-2513 4-1).
13
14
15
16
17
18
19
20
21
22
23
24
25
26
27
28
29
30
31
32
33
34
35
36
37
38
39
40
41
42
43
44
45
46
47
48
49
50
51
52
53
54
55
56
57
58
59
60
61
62
63
64
65

- 1 375 [1] J. Hasan, R.J. Crawford, E.P. Ivanova, *Trends Biotechnol.* **2013**, *31*, 295.
- 2 376 [2] M.L.W. Knetsch, L.H. Koole, *Polymers* **2011**, *3*, 340.
- 3 377 [3] S.R. Shah, A.M. Tataru, R.N. D'Souza, A.G. Mikos, F.K. Kasper, *Materials Today*
- 4 378 **2013**, *16*, 177.
- 5 379 [4] P. Basak, B. Adhikari, I. Banerjee, T.K. Maiti, *J Mater Sci Mater Med* **2009**, *20 Suppl*
- 6 380 *1*, S213.
- 7 381 [5] I. Francolini, L. D'Ilario, E. Guaglianone, G. Donelli, A. Martinelli, A. Piozzi, *Acta*
- 8 382 *Biomater* **2010**, *6*, 3482.
- 9 383 [6] R.D. Boyd, J. Verran, M.V. Jones, M. Bhakoo, *Langmuir* **2002**, *18*, 2343.
- 10 384 [7] K.A. Whitehead, J. Verran, *Food and Bioproducts Processing* **2006**, *84*, 253.
- 11 385 [8] K.A. Whitehead, D. Rogers, J. Colligon, C. Wright, J. Verran, *Colloids Surf B*
- 12 386 *Biointerfaces* **2006**, *51*, 44.
- 13 387 [9] B. Park, V. Nizet, G.Y. Liu, *J Bacteriol* **2008**, *190*, 2275.
- 14 388 [10] S. Abban, M. Jakobsen, L. Jespersen, *Food Microbiol.* **2012**, *31*, 139.
- 15 389 [11] N. Mitik-Dineva, J. Wang, V.K. Truong, P. Stoddart, F. Malherbe, R.J. Crawford, E.P.
- 16 390 Ivanova, *Curr. Microbiol.* **2009**, *58*, 268.
- 17 391 [12] A. Biswas, I.S. Bayer, A.S. Biris, T. Wang, E. Dervishi, F. Faupel, *Adv Colloid*
- 18 392 *Interface Sci* **2012**, *170*, 2.
- 19 393 [13] P. Kim, A.K. Epstein, M. Khan, L.D. Zarzar, D.J. Lipomi, G.M. Whitesides, J.
- 20 394 Aizenberg, *Nano Lett.* **2012**, *12*, 527.
- 21 395 [14] M.V. Graham, A.P. Mosier, T.R. Kiehl, A.E. Kaloyeros, N.C. Cady, *Soft Matter* **2013**,
- 22 396 *9*, 6235.
- 23 397 [15] K. Manabe, S. Nishizawa, S. Shiratori, *ACS Appl Mater Interfaces* **2013**, *5*, 11900.
- 24 398 [16] M. Graham, N. Cady, *Coatings* **2014**, *4*, 37.
- 25 399 [17] M. Bieda, C. Schmädicke, T. Roch, A. Lasagni, *Adv. Eng. Mater.* **2014**, n.
- 26 400 [18] J.W. Costerton, P.S. Stewart, E.P. Greenberg, *Science* **1999**, *284*, 1318.
- 27 401 [19] G. O'Toole, H.B. Kaplan, R. Kolter, *Annu Rev Microbiol* **2000**, *54*, 49.
- 28 402 [20] L. Hall-Stoodley, P. Stoodley, *Curr Opin Biotechnol* **2002**, *13*, 228.
- 29 403 [21] L. Hall-Stoodley, P. Stoodley, *Trends in Microbiology* **2005**, *13*, 7.
- 30 404 [22] F. Götz, *Curr Opin Microbiol* **2004**, *7*, 477.
- 31 405 [23] D. Langheinrich, E. Yslas, M. Broglia, V. Rivarola, D. Acevedo, A. Lasagni, *J. Polym.*
- 32 406 *Sci. B Polym. Phys.* **2011**, *50*, 415.
- 33 407 [24] J. Valle, A. Toledo-Arana, C. Berasain, J.-M. Ghigo, B. Amorena, J.R. Penadés, I.
- 34 408 Lasa, *Mol Microbiol* **2003**, *48*, 1075.
- 35 409 [25] J.M. Ghigo, *Nature* **2001**, *412*, 442.
- 36 410 [26] T.J. Foster, J.A. Geoghegan, V.K. Ganesh, M. Höök, *Nat Rev Micro* **2014**, *12*, 49.
- 37 411 [27] M. Katsikogianni, Y.F. Missirlis, *Eur Cell Mater* **2004**, *8*, 37.
- 38 412 [28] L.-C. Xu, C.A. Siedlecki, *Acta Biomater* **2012**, *8*, 72.
- 39 413 [29] L.C. Hsu, J. Fang, D.A. Borca-Tasciuc, R.W. Worobo, C.I. Moraru, *Appl Environ*
- 40 414 *Microbiol* **2013**, *79*, 2703.
- 41 415 [30] R.S. Friedlander, H. Vlamakis, P. Kim, M. Khan, R. Kolter, J. Aizenberg, *Proceedings*
- 42 416 *of the National Academy of Sciences* **2013**.
- 43 417 [31] K.A. Whitehead, J. Colligon, J. Verran, *Colloids Surf B Biointerfaces* **2005**, *41*, 129.
- 44 418 [32] C. Díaz, M. Cortizo, P. Schilardi, *Materials Research* **2007**, *10*, 11.
- 45 419 [33] S. Rozhok, Z. Fan, D. Nyamjav, C. Liu, C.A. Mirkin, R.C. Holz, *Langmuir* **2006**, *22*,
- 46 420 *11251*.
- 47 421 [34] T. Scheuerman, A. Camper, M. Hamilton, *J Colloid Interface Sci* **1998**, *208*, 23.
- 48 422 [35] C. Díaz, P.L. Schilardi, R.C. Salvarezza, M.F.L. de Mele, *Langmuir* **2007**, *23*, 11206.
- 49 423 [36] S. Hou, H. Gu, C. Smith, D. Ren, *Langmuir* **2011**, *27*, 2686.
- 50 424 [37] K.K. Chung, J.F. Schumacher, E.M. Sampson, R.A. Burne, P.J. Antonelli, A.B.

425 Brennan, *Biointerphases* **2007**, 2, 89.

426 [38] A.S.F. Lasagni, **2012**, 1.

1 427 [39] K. Modjarrad, S. Ebnesajjad *Handbook of Polymer Applications in Medicine and*
2 428 *Medical Devices*, Amsterdam : Elsevier/William Andrew, **2013**

3 429 [40] L. Müller-Meskamp, Y.H. Kim, T. Roch, S. Hofmann, R. Scholz, S. Eckardt, K. Leo,
4 430 A.F. Lasagni, *Adv. Mater. Weinheim* **2012**, 24, 906.

5 431

6 432

7

8

9

10

11

12

13

14

15

16

17

18

19

20

21

22

23

24

25

26

27

28

29

30

31

32

33

34

35

36

37

38

39

40

41

42

43

44

45

46

47

48

49

50

51

52

53

54

55

56

57

58

59

60

61

62

63

64

65

433 **Table 1. Description of polymeric materials modified by DLIP**

434

435

436

437

438

439

440

441

442

443

444

445

Polymeric material	Λ = period (μm)	Topography	F = Fluence (J/cm^2)
PS	5	Line (LN)	0.5
PS	5	Pillar (PL)	0.5
PS	3	Line (LN)	0.5
PS	3	Pillar (PL)	0.5
PS	1	Line (LN)	0.5
PS	1	Pillar (PL)	0.5
PS	5	Lamella (LA)	0.5
PS	2	Lamella (LA)	0.5
PS	-	Non-patterned (CT)	-

1
2
3
4
5
6
7
8
9
10
11
12
13
14
15
16
17
18
19
20
21
22
23
24
25
26
27
28
29
30
31
32
33
34
35
36
37
38
39
40
41
42
43
44
45
46
47
48
49
50
51
52
53
54
55
56
57
58
59
60
61
62
63
64
65

446

1 447

2

3 448

4

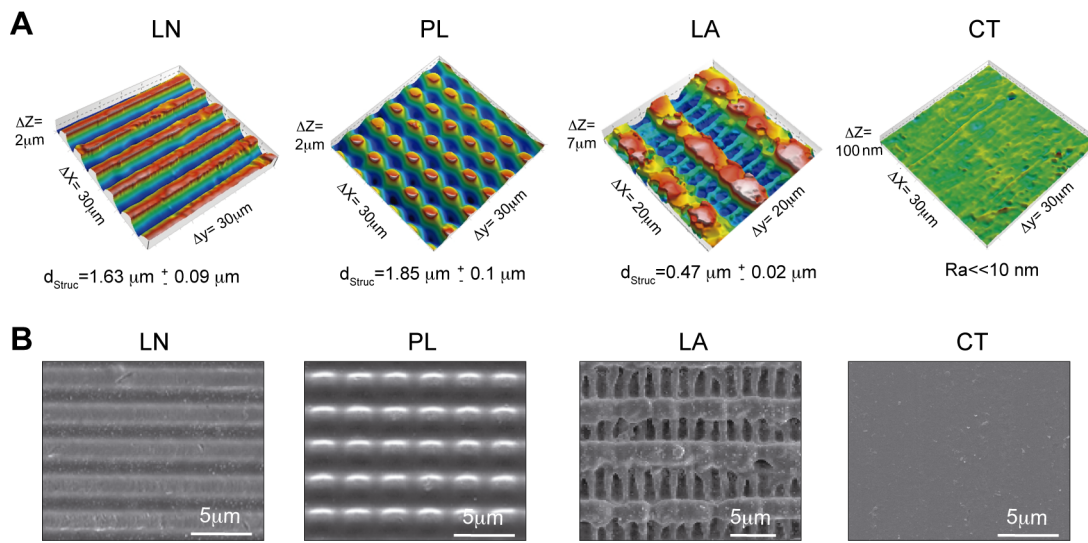
5 449

6

7 450

8

9 451



10 451

11

12 452

13

14 453

15

16 454

17

18 455

19

20 456

21

22 457

23

24 458

25

26 459

27

28

29

30

31

32

33

34

35

36

37

38

39

40

41

42

43

44

45

46

47

48

49

50

51

52

53

Figure 1: Images from confocal (A) and scanning electron microscopy (B) of PS polymeric surfaces structured by Direct Laser Interference Patterning technique. Periodic arrays of line-like (LN, $\Lambda = 5 \mu\text{m}$), pillar-like (PL, $\Lambda = 5 \mu\text{m}$), lamella-like (LA, $\Lambda = 2 \mu\text{m}$) structures and non-modified surfaces (CT). The laser fluence was kept constant at 0.5 J cm^{-2} .

460

1 461

2

3 462

4

5 463

6

7 464

8

9 465

10

11 466

12

13 467

14

15 468

16

17 469

18

19

20

21

22

23 470

24

25 471

26

27 472

28

29 473

30

31 474

32

33 475

34

35 476

36

37

38

39

40

41

42

43

44

45

46

47

48

49

50

51

52

53

54

55

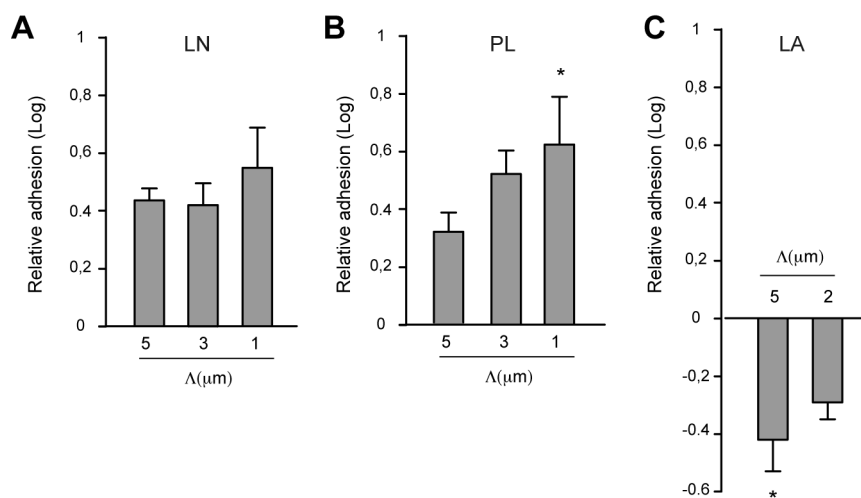
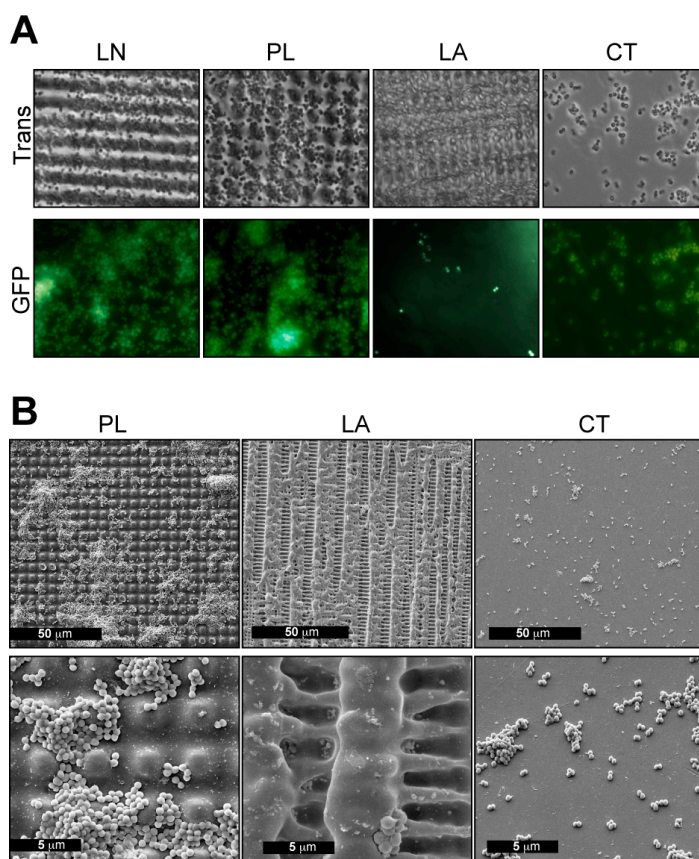


Figure 2. Bacterial adhesion on patterned surfaces under static conditions. Relative adhesion of *S. aureus* on PS patterned surfaces with line (LN) (A), pillar (PL) (B), and lamella-like (LA) (C) structures and with spatial periods (Λ) of 1, 2, 3 and 5 μm . Relative adhesion was calculated as bacterial counts CFU on patterned surfaces / CFU on non-patterned surfaces. Multiple comparisons were performed by one-way analysis of variance combined with the Bonferroni multiple comparison test (GraphPad Instat, version 5). Asterisk indicates significant adhesion differences (*, $P < 0.05$ [significant]). ns, non significant differences.

477



1 478

2 479

3 480

4 481

5 482

6 483

7 484

8 485

9 486

10 487

11 488

12 489

13 **Figure 3:** Qualitative evaluation of *S. aureus* attachment to patterned PS wafers. A)

14 Fluorescence microscopic images of *S. aureus* 15981-GFP attached to PL, LN, LA and non-

15 patterned PS surfaces (CT), showing preferential positioning relative to surface topography. B)

16 Scanning electron micrographs of *S. aureus* cells attached to PL, LA and non-patterned PS

17 surfaces (CT).

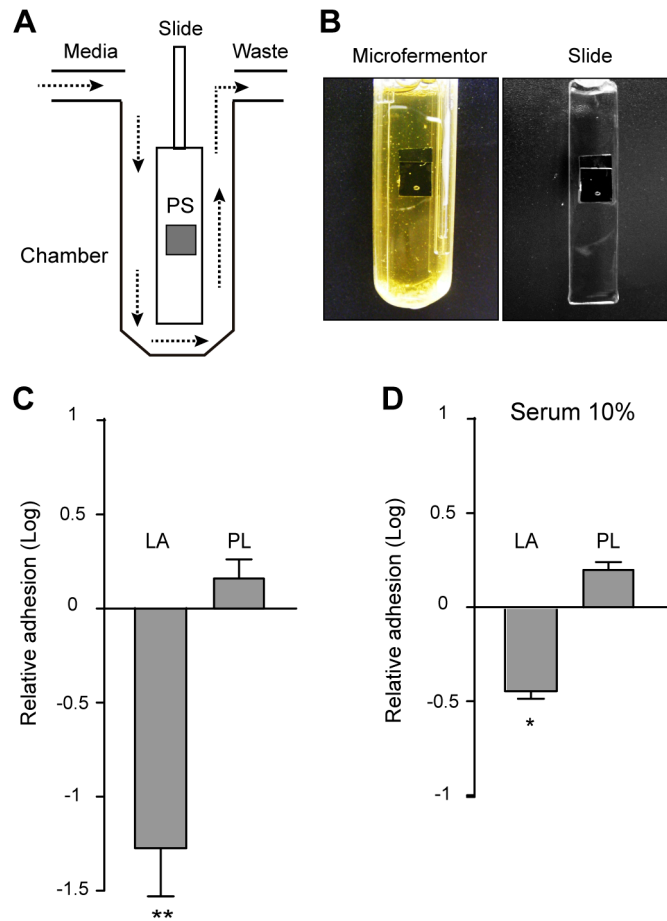
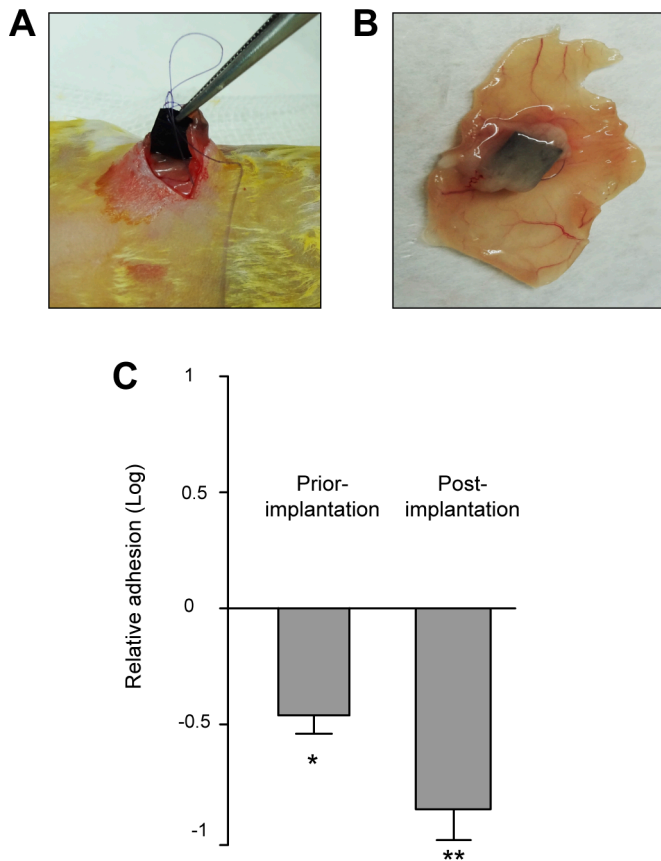


Figure 4: Bacterial adhesion on patterned surfaces in microfermenters. Schematic diagram (A) and photograph image taken from the microfermenters (B). Substrates of 1x1 cm² were fixed on the glass slide. Microfermenters were inoculated with *S. aureus* 15981 (OD_{600nm}=1). After 6 hours of incubation, substrates were removed from the glass slide and quantification of adhered *S. aureus* cells was performed by CFU counting of the bacteria removed from the tested surfaces. Graphs show the relative adhesion of *S. aureus* on LA, PL and non-patterned (CT) PS surfaces under flow culture conditions in the absence (C) or presence of human serum (D). Relative adhesion was calculated as bacterial counts CFU on patterned surfaces / CFU on non-patterned surfaces. Comparisons were performed by one-way analysis of variance combined with the Bonferroni multiple comparison test or Mann-Whitney test (GraphPad InStat, version 5)

519



520

521

522

523

524

525

526

527

528

529

530

531

532

533 **Figure 5:** Biofilm formation of *S. aureus* on lamella-like patterned surfaces using an *in vivo*

534 model. A) Implantation of substrates in the intraperitoneal cavity of CD1 mice. B) Biofilm-

535 infected surfaces after 5 days of infection. C) Contamination of PS polymers prior-

536 implantation: PS lamella-like and control surfaces were first coated with 10^4 cfu of *S. aureus*

537 15981 and then fixed at the abdominal wall. Contamination of PS polymers post-implantation:

538 PS polymers were first fixed at the abdominal wall before infection. Two day after implantation

539 a 10^8 cfu of *S. aureus* 15981 were injected intraperitoneally at the site of the implant. After 5

540 days, animals (n=6) of both types of infections were sacrificed and substrates were extracted

541 and placed in 1 ml of PBS. Samples were serially diluted and plated onto TSA plates for

542 enumeration of viable staphylococci.

543